http://www.zju.edu.cn/jzus; E-mail: jzus@zju.edu.cn
ISSN 1009 – 3095 *Journal of Zhejiang University SCIENCE* V.5, No.1, P.111 – 116, Jan., 2004

Sedimentation of a single particle between two parallel walls*

SHAO Xue-ming(邵雪明)†1, LIN Jian-zhong(林建忠)[1], YU Zhao-sheng(余钊圣)[2]

([1] *Department of Mechanics, Zhejiang University, Hangzhou 310027, China*)

([2] *Department of Mechanical and Mechatronic Engineering, the University of Sydney, NSW 2006, Australia*)

†E-mail: mecsxm@public.zju.edu.cn

Received Nov.4, 2002; revision accepted Feb.19, 2003

Abstract: The sedimentation of a single circular particle between two parallel walls was studied by means of direct numerical simulation (DNS) and experiment. The improved implementation of distributed Lagrange multiplier/fictitious domain method used in our DNS is a promising new way for simulation of particulate flows. The settling behaviors of the particle are presented ranging in Reynolds number from 0 to about 700, which showed that our results for low Reynolds numbers agreed well with that reported before. Nevertheless, for higher Reynolds numbers our results were different from theirs. The long-term mean equilibrium positions in our results were all on the centerline, but not at off-center position as reported before. In order to validate our simulation, experiments were also conducted. The results showed that the sedimenting behavior simulated in this paper agreed well with our experiment result.

Key words: Sedimentation, Circular particle, Distributed Lagrange multiplier/fictitious domain method

Document code: A **CLC number:** O359

INTRODUCTION

The centering of a particle which settles at small Reynolds numbers had been studied by several researchers. Christopherson and Dowson (1959) found that theoretically, when the effect of inertia is negligible, a ball achieves eccentric equilibriun in a vertical tube having a diameter only slightly exceeding the diameter of the ball. They verified their analysis with experiments. Vaseur and Cox (1977) did experiments on the sedimentation of a small sphere in a vertical duct of a rectangular cross-section. They observed that the sphere always migrated to the center-plane of the two vertical walls when the Reynolds number was small. Tachibana (1973), working with spheres settling in a vertical round pipe, observed a similar phenomenon at $Re = 0.093$. Perfect centering of cylinders falling in viscoelastic liquids between the closely spaced sidewalls was observed by Joseph and Liu, if the settling velocities were not very slow.

On the other hand, the settling behavior of particle at high Reynolds numbers has been little studied. Feng *et al*. (1994) simulated the settling of a single ciucular particle through quiescent fluid between parallel walls by using a Navier-Stokes slover-POLYFLOW based on unstructured grids (Hu *et al*., 1992). The behavior of a particle in a channel is classified into five different regimes which occur at different Reynolds number intervals depending on the channel width. The trajectories of the particle were presented up to $Re = 575$. But to our knowledge, no systematic experimental work on the settling of a particle at high Reynolds numbers has been reported. Feng *et al*. (1994) also mentioned that the only verification of the irregular oscillation of a particle at high Reynolds number is Tachibana's (1973) experiment on the settling behavior of a sphere in a vertical round pipe. However, their results (that the mean equilibrium which is away from the centerline at high Reynolds number) was not verified.

* Project supported by the National Natural Science Foundation of China (No. 19925210) and Zhejiang Provincial Natural Science Foundation (No. 101047)

Our goal in this work is to re-examine this interesting problem with an improved implementation of the distributed Lagrange multiplier/fictitious domain method, and compare the simulated results with our experiments on the settling of a 'two-dimensional' column with high aspect ratio.

Particulate flows of solids in fluids are widely used for different purposes in different industries (Lin *et al*., 2002). Among the practical applications without complicating features, many are suitable for direct simulation. The distributed Lagrange multiplier/fictitious domain method is a promising new way for the direct numerical simulation of particulate flows, by which the Navier-Stokes equations governing the motion of the fluids and the equations of rigid-body motion governing the motion of the particles are solved simultaneously without any approximations. Its basic idea (Glowinski *et al*., 1999) is to extend the problem on a geometrically complex (possibly time-dependent) domain to a larger, simpler domain (the "fictitious domain"), and the fluid-particle motion is treated implicitly via a combined weak formulation in which the constraint of rigid-body motion is enforced as a side constraint using a distributed Lagrange multiplier. According to this method, explicit calculation of the hydrodynamic forces and torques on the particles is no longer required, and a fixed structured mesh can be used for the entire computation, which eliminates the need for repeated remeshing and projection, and allows efficient parallel algorithm and fast solution methods to be implemented. This is a great contrast to the scheme based on moving unstructured grids (Patankar, 1997; Glowinski *et al*., 2001).

NUMERICAL METHOD

Equations of motion

In this paper, we will focus on the motion of circular particles in two-dimensional flows. The schematic of the computational domain is shown in Fig. 1. For simplicity, we assume that the entire computational domain Ω is a rectangle with boundary $\Gamma = \bigcup_{i=1}^{4} \Gamma_i$. The interior of the ith particle is presented by $P_i(t)$, 1, ..., N.

The motion of fluid and particles is governed by the following equations.

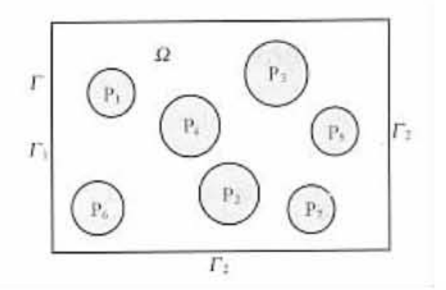

Fig.1 The schematic of computational domain

Fluid motion

$$\rho_L\left[\frac{\partial \boldsymbol{u}}{\partial t} + (\boldsymbol{u}\cdot\nabla)\boldsymbol{u}\right] = \rho_L \boldsymbol{g} + \nabla\cdot\sigma \quad \text{in } \Omega \setminus \overline{P(t)}, \tag{1}$$

$$\nabla\cdot\boldsymbol{u} = 0 \quad \text{in } \Omega \setminus \overline{P(t)}, \tag{2}$$

$$\sigma = -p\boldsymbol{I} + 2\eta\boldsymbol{D}[\boldsymbol{u}] \quad \text{for Newtonian fluid}, \tag{3}$$

$$\boldsymbol{u} = \boldsymbol{u}_\Gamma(t) \quad \text{on } \Gamma, \tag{4}$$

$$\boldsymbol{u} = \boldsymbol{U}_i + \omega_i \times \boldsymbol{r}_i \quad \text{on } \partial P_i(t), \quad i = 1, \cdots, N, \tag{5}$$

$$\boldsymbol{u}\mid_{t=0} = \boldsymbol{u}_0 \quad \text{in } \Omega \setminus \overline{P(0)}. \tag{6}$$

Particle motion

$$M_i \frac{\mathrm{d}\boldsymbol{U}_i}{\mathrm{d}t} = M_i\boldsymbol{g} + \boldsymbol{F}_i + \boldsymbol{F}_i', \tag{7}$$

$$I_i \frac{\mathrm{d}\omega_i}{\mathrm{d}t} = T_i, \tag{8}$$

$$\boldsymbol{U}_i \mid_{t=0} = \boldsymbol{U}_{i,0}, \tag{9}$$

$$\omega_i \mid_{t=0} = \omega_{i,0}. \tag{10}$$

Kinematic equations

$$\frac{\mathrm{d}\boldsymbol{X}_i}{\mathrm{d}t} = \boldsymbol{U}_i, \tag{11}$$

$$\frac{\mathrm{d}\Theta_i}{\mathrm{d}t} = \omega_i, \tag{12}$$

$$\boldsymbol{X}_i \mid_{t=0} = \boldsymbol{X}_{i,0}, \tag{13}$$

$$\Theta_i \mid_{t=0} = \Theta_{i,0}. \tag{14}$$

Here, $\boldsymbol{u}$, p, η, ρ_L, $\boldsymbol{D}$ and σ are the fluid velocity, pressure, viscosity, density, the rate of deformation tensor, and the stress tensor. $\boldsymbol{r}_i = \boldsymbol{x} - \boldsymbol{X}_i$ is the position from the center of particle i. M_i, I_i, $\boldsymbol{U}_i$, ω_i, Θ_i, and $\boldsymbol{X}_i$ are the mass, moment of inertia, translational velocity, angular velocity, angular orientation and centre of mass of particle i. $\boldsymbol{F}_i$ and T_i are the force and torque acting on the particle i. $\boldsymbol{F}_i'$ is the artificial repulsive force exerted on the ith particle by the other particles and walls at close range to prevent particles from penetrating each other or the four walls. In our simulation, $\boldsymbol{F}_i'$ is set to be directly proportional to relative velocity between particles.

Weak form

As mentioned above, the basic idea of the DLM method is to extend the problem on a geometrically complex domain to a larger, simpler domain, and to treat the fluid-particle motion implicitly via a combined weak formulation in which the constraint of rigid-body motion is enforced as a side constraint using a distributed Lagrange multiplier. The detailed derivation of this weak form is omitted due to the limit of pages. For simplicity, only one particle is considered in the following presentation. The extension to the many-particle case is straightforward.

For a.e. $t > 0$, find $\boldsymbol{u} \in W_{\boldsymbol{u}_\Gamma}$, $p \in L_0^2(\Omega)$, $\lambda \in \Lambda(t)$, $\boldsymbol{U} \in \boldsymbol{R}^2$, and $\omega \in \boldsymbol{R}$, satisfying

$$\int_\Omega \rho_L \left[\frac{\partial \boldsymbol{u}}{\partial t} + (\boldsymbol{u} \cdot \nabla)\boldsymbol{u} - \boldsymbol{g}\right] \cdot \boldsymbol{v} \mathrm{d}\boldsymbol{x} - \int_\Omega p \nabla \cdot \boldsymbol{v} \mathrm{d}\boldsymbol{x} + \int_\Omega 2\eta \boldsymbol{D}[\boldsymbol{u}] : \boldsymbol{D}[\boldsymbol{v}] \mathrm{d}\boldsymbol{x} + \left(1 - \frac{\rho_L}{\rho_d}\right)\left[M\left(\frac{\mathrm{d}\boldsymbol{U}}{\mathrm{d}t} - \boldsymbol{g}\right) \cdot \boldsymbol{V} + I\frac{\mathrm{d}\omega}{\mathrm{d}t}\xi\right] - \boldsymbol{F}' \cdot \boldsymbol{V} = \langle \lambda, \boldsymbol{v} - (\boldsymbol{V} + \xi \times \boldsymbol{r})\rangle_{P(t)}$$

for all $\boldsymbol{v} \in W_0$, $\boldsymbol{V} \in \boldsymbol{R}^2$, and $\xi \in \boldsymbol{R}$, (15)

$$\int_\Omega q \nabla \cdot \boldsymbol{u} \mathrm{d}\boldsymbol{x} = 0 \quad \text{for all } q \in L^2(\Omega), \tag{16}$$

$$\langle \mu, \boldsymbol{u} - (\boldsymbol{U} + \omega \times \boldsymbol{r})\rangle_{P(t)} = 0 \quad \text{for all } \mu \in \Lambda(t), \tag{17}$$

$$\boldsymbol{u}\,|_{t=0} = \boldsymbol{u}_0 \quad \text{in } \Omega \tag{18}$$

as well as the kinematic Eqs. (11), (12) and the initial condition for the particle translational and angular velocities Eq.(9), Eq.(10). Here

$$W_{\boldsymbol{u}_\Gamma} = \{\boldsymbol{v} \in H^1(\Omega)^2 \mid \boldsymbol{v} = \boldsymbol{u}_\Gamma(t) \text{on } \Gamma\}$$

$$W_0 = \{\boldsymbol{v} \in H^1(\Omega)^2 \mid \boldsymbol{v} = 0 \text{ on } \Gamma\}$$

$$L_0^2(\Omega) = \{q \in L^2(\Omega) \mid \int_\Omega q \mathrm{d}\boldsymbol{x} = 0\}$$

and $\Lambda(t)$ is an appropriate space by which the constraint of rigid-body motion inside particle is enforced. For the inner product $\langle \cdot, \cdot \rangle$ on $\Lambda(t)$, we will use the following form in this paper.

$$\langle \mu, \boldsymbol{v} \rangle_{p(t)} = \int_{p(t)} \mu \cdot \boldsymbol{v} \mathrm{d}\boldsymbol{x} \tag{19}$$

Computational scheme

In this paper, a rectangular discretization for velocity and pressure are used as shown in Fig. 2. We adopt the so-called "Q_1-P_0" element, namely, the velocity is made of piecewise polynomials and the pressure is piecewise constant on a rectangular grid. The key feature of this rectangular scheme is that it has good symmetry property and pressure has almost the same degree as the velocity. The scheme works well in our numerical simulation as discussed in the following section. Compared to the triangular scheme, it allows the solution to satisfy better the incompressibility condition and can give a more accurate simulation of the motion of particles, especially at moderate and high Reynolds number.

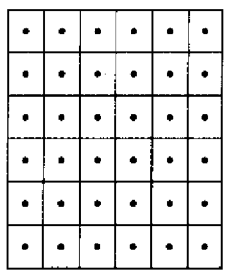

Fig.2 Velocity and pressure mesh (• represents pressure discretization point)

For time discretization, the Marchuk-Yanenko operator splitting scheme is used to solve the initial value problem Eqs. (15) – (18). This scheme allows decoupling of the principal numerical difficulties including the incompressibility condition, the advection and diffusion terms and the constraint of rigid-body motion in $p_h(t)$.

In addition, the buoyant force is considered while predicting the position of particles at a new time step in our scheme. This improved the accuracy for the prediction of the particle's positions, particularly when ρ_d is nearly equal to ρ_L.

RESULTS AND DISCUSSION

We now discuss the results obtained using the above algorithm for the motion of a circular particles settling in a two-dimensional channel filled with Newtonian fluid. In our numerical simulations discussed here, we assume that all dimensional quantities are in CGS units.

Simulation results

According to Feng *et al*. (1994) simulated results, the lateral migration behavior of a settling circular particle between two parallel walls with width $L = 4D$ (D is the diameter of the particle) is classified into five regimes which occur at different Reynolds number intervals. In regime A ($0.1 < Re < 2$), the particle drifts monotonically to a steady equilibrium on the centreline of the channel independent of the initial position of the particle. In regime B ($3 < Re < Re_{crit}$), the centre of the channel is still the equilibrium position, but the approach to it is not monotonic. There is an initial overshoot followed by a damped oscillation. In regime C ($Re_{crit} < Re < 60$), the steady equilibrium position at the centre of the channel becomes unstable, and the long-term behavior of the particle is a weak oscillation around an equilibrium position slightly off-centre. In regime D ($60 < Re < 300$), the particle oscillates with much larger amplitude around a mean equilibrium position that is further away from the centreline. In regime E ($Re > 300$), the behavior of the particle becomes unstable and break down into less regular patterns.

In this work, the settling behaviors of a circular particle between two parallel walls were also studied at different Reynolds number with our DLM code. We first compared our computed drag coefficients with the standard drag and those by Feng *et al*. (1994) as shown in Fig.3. We note that our and Feng's results agree well with each other. This indicates that the accuracy of the DLM method to compute the streamwise velocities of the particle in a wide range of Reynolds numbers is good. In Fig. 3, The standard drag is an empirical correlation of experimental data on a fixed cylinder in an unbounded domain (Suker and Brauer, 1975). We note that the wall confinement generally decreases the settling velocity and inversely increases the drag coefficient of the particle; and that this effect decreases with Re.

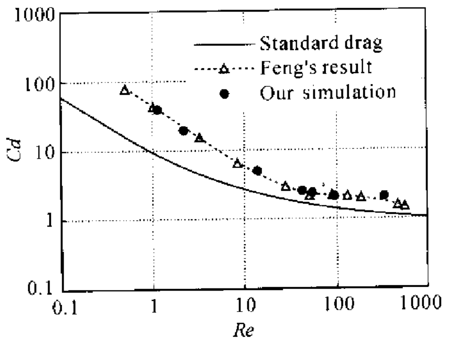

Fig.3 Drag coefficients of a particle settling in channels as compared to the standard drag and the numerical result of Feng *et al*.(1994)

The settling trajectories of the particle in our simulations are shown in Fig.4. We can see that the behaviors of the particle at low Reynolds numbers (Fig.4a and Fig.4b) agree well with the results (regime A and B) presented by Feng *et al*. (1994). Nevertheless, our results for the subsequent regimes are different from theirs. It is clear from Fig. 4 that the long-term mean equilibrium positions in our results (Figs. 4a, 4b, 4c) are all at the centerline, but not at off-center position as presented by Fent *et al*. (1994). We think that this difference does not conflict with the agreement of drag coefficient Cd as mentioned above, because the lateral migration and long-term equilibrium position of the particle are mainly determined by the wake of the particle and the interactions between particle and the walls.

As shown in Fig.4, the lateral migration behaviors at high Reynolds number in our simulations can be described as follows: For the case of $Re = 54.6$ (Fig. 4c), the particle sediments eventually along the centerline. It is the same as that presented in regime B. Nevertheless, the way in which the particle approaches the centerline is different from that in regime B. It consists of a monotonic approach to the centerline and a "wagging" movement caused by vortex shedding. For the case of $Re = 163.0$ (Fig.4d), the approach of the particle to the centerline is similar to that at $Re = 54.6$. The difference is that the particle sediments either eventually settle along the centerline, or oscillate regularly about the centerline at a constant frequency and amplitude. It is reasonable that, when the Reynolds number is higher than about 60, the wake vortices become unsteady and persistent vortex shedding can be observed. In our simulation, due to the confinement of the walls, the wake vortices line up vertically. For the case of $Re = 675.0$ (Fig.4e), the approach to the centerline is no longer monotonic. An initial overshoot can be observed again as that in regime B. The long-term behavior also is that the particle settles along the centerline and oscillates regularly about the centerline at a constant frequency and amplitude.

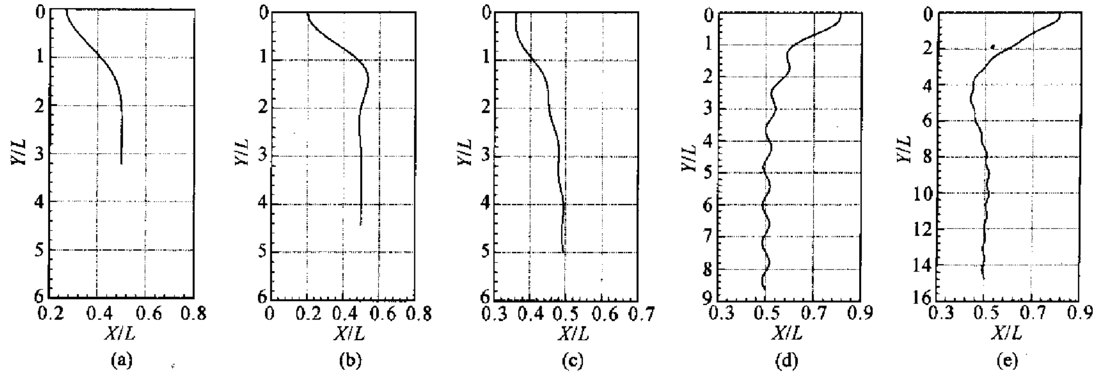

Fig.4 Simulation results: settling trajectories of a circular particle between two parallel walls
(a) $Re = 1.7$; (b) $Re = 13.4$; (c) $Re = 54.6$; (d) $Re = 163.0$; (c) $Re = 675.0$

Comparison with experimental results

In order to validate our simulation, we did experiments on the sedimentation of a 'two-dimensional' column with aspect ratio of 12 in a vertical duct of width $4D$. The cross-section of the duct was a rectangle with aspect ratio of 8 so that the effect of the two widely spaced walls might have been negligible. The fluid used in the duct was an aqueous solution of sirup, whose density and viscosity can be changed with the concentration of the sirup. So it was possible to make careful observation on the behavior of the column ranging in Reynolds number from 0 to about 1000. Fig. 5 shows the experimental results in which the trajectories of the column at different Reynolds numbers are presented. We can see that our simulated trajectories all compare well with the experiments at different regimes. The experimental results also showed that the mean equilibrium positions of the particle at

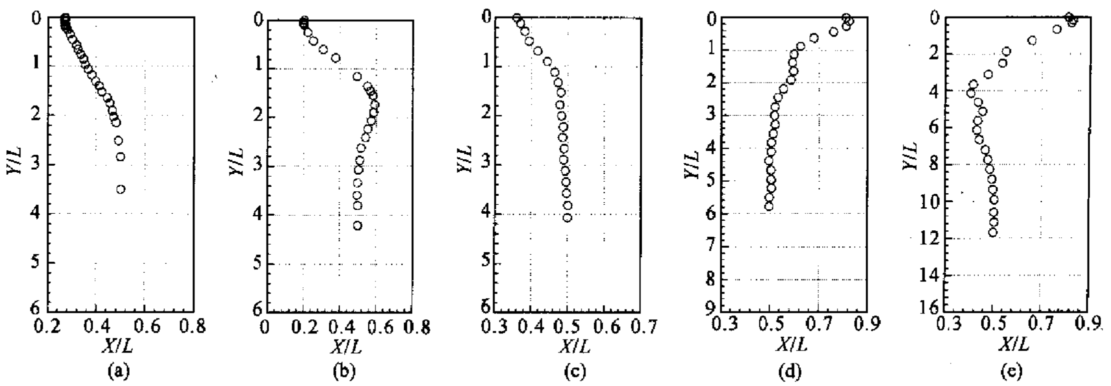

Fig.5 Experimental results: settling trajectories of a particle in a vertical duct
(a) $Re = 2.3$; (b) $Re = 11.4$; (c) $Re = 48.6$; (d) $Re = 161.6$; (e) $Re = 682.0$

all tested Reynolds numbers were at the centerline. Some typical features, such as the overshoot at $Re = 13.4$ and 675.0, the "wagging" movement when the particle approaches the centerline at $Re = 163.0$, were all correctly simulated although quantitative discrepancies exist for understandable reasons. This means that our DLM code can give a relatively more accurate simulation of the particle's motion.

CONCLUSIONS

According to Feng's simulation results, the settling behavior of a circular particle between two parallel walls is classified into five regimes which occur at different Reynolds number intervals. In this paper, this interesting problem is re-examined by means of direct numerical simulation (DNS) and experiment. The settling behaviors of the particle are presented ranging in Reynolds number from 0 to about 700. It was found that our results for low Reynolds numbers agreed well with results presented by Feng *et al*. (1994). Nevertheless, for higher Reynolds numbers our results were different from theirs. The long-term mean equilibrium positions in our results were all located at the centerline, but not at an off-center position as presented by Fent *et al*.(1994). In order to validate our simulation, the experiments on the sedimentation of a 'two-dimensional' column with aspect ratio of 12 in a vertical duct were also conducted. The result showed that the sedimenting behavior simulated in this paper agreed well with our experiment. The mean equilibrium positions of the particle at all tested Reynolds numbers were at the centerline.

References

Christonpherson, D. G. and Dowson, D., 1959, An example of minimum energy dissipation in viscous flow. *Proc. R. Soc.*, A251:550 – 564.

Feng, J., Hu, H. H. and Joseph, D. D., 1994. Direct simulation of initial value problems for the motion of solid bodies in a Newtonian fluid, Part 1. Sedimentation. *J. Fluid Mech.*, **261**: 95 – 134.

Glowinski, R., Pan, T. W., Hesla, T. I. and Joseph, D. D., 1999. A distributed Lagrange multiplier/fictitious domain methos for particulate flows. *Int. J. Multiphase Flow*, **25**: 755 – 794.

Glowinski, R., Pan, T. W., Hesla, T. I., Joseph, D.D. and Periaux, J., 2001. A fictitious domain approach to the direct numerical simulation of incompressible viscous flow past moving rigid bodies: Application to particulate flow. *J. Comp. Phys.*, **169**: 363 – 426.

Hu, H.H., Joseph, D.D. and Crochet, M.J., 1992. Direct simulation of fluid particle motions. *Theor. Comp. Fluid Dyn.*, **3**: 285 – 306.

Lin, J.Z., Zhang, W.F. and Wang, Y.L., 2002. Research on the orientation distribution of fibers immersed in a pipe flow. *J. Zhejiang Univ. Sci.*, **3**(5):501 – 506.

Patankar, N.A., 1997. Numerical simulation of particulate two-phase flow. Ph.D. thesis. University of Pennsylvania, Pennsylvania.

Suker, D. and Brauer, H., 1975. Fluiddynamik bei quer angeströmten Zylindern. *Wärme-und Stoffübertragung*, **8**:149 – 158.

Tachibana, M., 1973. On the behaviour of a sphere in the laminar tube flows. *Rheol. Acta*, **12**: 58 – 69.

Vasseur, P. and Cox, R. G., 1977. The lateral migration of spherical particles sedimenting in a stagnant bounded fluid. *J. Fluid Mech.*, **80**: 561 – 591.